

Water Resources Research

RESEARCH ARTICLE

10.1029/2019WR025030

Special Section:

Advances in remote sensing, measurement, and simulation of seasonal snow

Key Points:

- A nonlinear relationship between the mean and the standard deviation of snow depth is observed and modelled
- The shape of the distribution of snow depth changes with the mean snow depth
- The gamma distribution is the best-suited model for the spatial frequency distribution of snow depth

Correspondence to:

T. Skaugen,
ths@nve.no

Citation:

Skaugen, T., & Melvold, K. (2019). Modeling the snow depth variability with a high-resolution lidar data set and nonlinear terrain dependency. *Water Resources Research*, 55, 9689–9704, <https://doi.org/10.1029/2019WR025030>

Received 20 FEB 2019

Accepted 2 NOV 2019

Accepted article online 11 NOV 2019

Published online 23 NOV 2019

©2019. The Authors.

This is an open access article under the terms of the Creative Commons Attribution License, which permits use, distribution and reproduction in any medium, provided the original work is properly cited.

Modeling the Snow Depth Variability With a High-Resolution Lidar Data Set and Nonlinear Terrain Dependency

T. Skaugen¹  and K. Melvold¹

¹Hydrology Department, Norwegian Water Resources and Energy Directorate, Oslo, Norway

Abstract In the mountains of Norway, snow depth (SD) is highly variable due to strong winds and open terrain. To investigate snow conditions on one of Europe's largest mountain plateaus, Hardangervidda, we conducted snow measurement campaigns in spring 2008 and 2009 using airborne lidar scanning at the approximate time of annual snow maximum (mid-April). From 658 empirical distributions of SD at Hardangervidda, each comprised about 4,000 SD values sampled from a grid cell of 0.5 km², quantitative tests have shown that the gamma distribution is a better fit for SD than the normal and log-normal distributions. When aggregating snow and terrain data from 10 × 10 m to 0.5 km², we find that the standard deviation of the terrain parameter squared slope, land cover, and the mean SD are highly correlated (0.7, 0.52, and 0.89) to the standard deviation of SD. A model for SD variance is proposed that, in addition to addressing the dependencies between the variability of SD and the terrain characteristics, also takes into account the observed nonlinear relationship between the mean and the standard deviation of SD. When validated against observed SD variance retrieved from the same area, the model explains 81–83% of the observed variance for spatial scales of 0.5 and 5.1 km², which compares favorably to previous models. The model parameters can be determined from a GIS analysis of a detailed digital terrain and land cover model and will hence not increase the number of calibration parameters when implemented in environmental models.

Plain Language Summary Using airborne laser, 400 million snow depth measurements at Hardangervidda in Southern Norway have been collected. The amount of data has made in-depth studies of the spatial distribution of snow and its interaction with the terrain and vegetation possible. We find that the terrain variability, expressed by the square slope, the average amount of snow, and whether the terrain is vegetated or not, largely explains the variation of snow depth. With this information it is possible to develop equations that predict snow depth variability that can be used in environmental models, which again are used for important tasks such as flood forecasting and hydropower planning. One major advantage is that these equations can be determined from the data that are, in principle, available everywhere, provided there exists a detailed digital model of the terrain.

1. Introduction

Snow is an integral component of the hydrologic, ecological, and atmospheric systems in many countries. In Norway 30% of annual precipitation falls as snow, and in the mountain areas, as much as 50–60%. Knowledge of snow amounts and its spatial distribution is necessary for the prediction of water availability and the timing of snowmelt rates and runoff, which are important for spring melt floods, hydropower production planning, and water resource management. In addition, the spatial features of snow are crucial for avalanche warning/formation, reliable simulations of the energy, and mass exchange between land and the atmosphere, ecology (plants and animal life), and the spatial extent and degree of permafrost (Gisnås et al., 2016).

The complex interaction between spatially variable precipitation, topography, wind, radiation, and vegetation shapes the spatial variability of the accumulation and melting of snow. In addition, these processes act on different spatial scales ranging from tens to thousands of meters (e.g., Blöschl, 1999; Elder et al., 1991; Liston et al., 2007), so both representative sampling and the modeling of snow are challenging tasks.

A multitude of physically and empirically based models are used for predicting the amount of snow and its spatial distribution. Some models operate on a fine-resolution grid scale (ranging from points, a few meters

to hundreds of meters) (see, e.g., Brun et al., 1992; Liston & Elder, 2006) attempting to include a detailed, multilayered and physically based process representation. These models require fine-resolution meteorological and terrain data and are hence demanding in information need and computation time. Other models are typically more lumped in their approach where the aim is to represent the spatial distribution of snow over areas of some extent (catchments or elevation zones of catchments) through the use of probability distribution functions (PDFs). In such models, that is, catchment hydrological models, an estimate of the frequency of snow amounts over an area is more important than their exact location.

Many studies have shown that a realistically modeled spatial distribution of snow depth (SD) is important for the assessment of snow-covered area and, using the snow bulk density, to monitor the seasonal development of water resources (Buttle & McDonnell, 1987; Essery & Pomeroy, 2004; Liston et al., 1999; Luce et al., 1999; Luce & Tarboton, 2004). Based on observations, studies have shown that the SD distribution, especially at the time of maximum accumulation, can be approximated by a two-parameter log-normal distribution (Donald et al., 1995; Sælthun, 1996), a two-parameter gamma distribution (Kolberg & Gottschalk, 2010; Kuchment & Gelfan, 1996; Skaugen, 2007; Skaugen & Randen, 2013), or a normal distribution (Marchand & Killingtonveit, 2004, 2005). Helbig et al. (2015) investigated the spatial PDF of SD for three large alpine areas close to the time of maximum snow and found that the gamma and the normal distributions were better suited than the log-normal distribution. Similar results were also found by Winstral and Marks (2014) who investigated 11 years of snow data from a semiarid intermountain watershed. In order to determine the appropriate shape of the PDF of SD, one is obliged to estimate its statistical moments (the mean and variance suffice for a two-parameter distribution). Liston (2004) related fixed statistical moments of the PDF of SD to terrain variability, air temperature, and wind. However, López-Moreno et al. (2015) found differences in the spatial coefficient of variation (CV) of SD for low (high CV) and high (low CV) spatial average SD, and Alfnes et al. (2004), Skaugen (2007), and Skaugen and Randen (2013) demonstrated through the repeated measurements of the same snow course during the accumulation and melting seasons that the spatial PDF of SD changed its shape continuously. The shape evolves from skewed (high CV) at the beginning of the accumulation season, to a more symmetrical distribution as the accumulation proceeds (low CV) and to a more skewed again (high CV) as the snow melts. The latter three Norwegian studies reported on snow water equivalent (SWE) but used the average snow density measured twice during the snow course to calculate SWE from SD. The inferences on the distribution of SWE hence also apply to SD.

Many field-based studies have investigated the relationship between SD variability and small-scale terrain parameters and vegetation type (see Clark et al., 2011, for a comprehensive review of recent literature), potential solar radiation (López-Moreno et al., 2015), or just to the mean SD (Egli & Jonas, 2009; Egli et al., 2011; Pomeroy et al., 2004). Linear or multilinear regression models and binary regression tree models have been used to relate the mean, the standard deviation, or the CV of SD to terrain parameters (e.g., slope, aspect, and elevation). Typically, these types of models can explain about 18% to 91% of SD variability (Grünwald et al., 2013). The models are often site specific and thus not transferable to other sites with other characteristics. Grünwald et al. (2013) used multiple linear regression to examine SD data from several mountainous areas around the world. Results from this study show good model performance at each site, but a global model containing all data sets could only explain 23% (or 30% excluding catchments with glaciers) of the variability. Grünwald et al. (2013) therefore argued that SD and terrain are less universally related than as hypothesized by Lehning et al. (2011), and the application of a global model is limited. The performance of the linear regression model is dependent on the spatial scale, or support, of the data for which the model is developed. Jost et al. (2007) showed, for example, that the performance of their model decreased if individual snow samples were used instead of plot averaged values. Similar results were also found in Grünwald et al. (2013). At the very small scale, simple local terrain characteristics have been unable to explain the SD distribution (Deems et al., 2006; Grünwald et al., 2010; Grünwald et al., 2013; Trujillo et al., 2009). Much of the fine-scale snow variability may be a result of small-scale terrain effects that are not captured by the terrain parameters derived from adjacent grid points in a digital terrain model (DTM) (Grünwald et al., 2013; Jost et al., 2007).

One of the reasons for the quite substantial volume of studies discussing the appropriate spatial frequency distribution of snow is the difficulty of retrieving data sets of sufficient magnitude to estimate PDFs with a reasonable certainty. This is especially problematic in areas where wind is a dominant influence on snow distribution, as in mountains, tundra, and shrublands (Elder et al., 1991; Hiemstra et al., 2002; Liston & Sturm, 2002; Marchand & Killingtonveit, 2004; Schirmer et al., 2011; Sturm, Liston, et al., 2001; Sturm,

McFadden, et al., 2001). The large spatial variability in SD and SWE in alpine catchments makes it difficult to obtain representative SD data by traditional measurement techniques (Anderton et al., 2004; Elder et al., 1991; Erickson et al., 2005) since extensive measurement designs with a large number of snow courses are required (e.g., Elder et al., 2009). In recent years the advances in laser ranging technology (LiDAR) both airborne LiDAR (AL) and terrestrial LiDAR together with digital photogrammetry offer powerful tools for SD measurements in both alpine and forest areas and several studies have used these techniques (e.g., Deems et al., 2006; Hopkinson et al., 2004). These relative new techniques give reliable, high-quality, high-spatial-resolution, and accurate SD information and thus allow for analyzing the distribution of SD over multiple scales (e.g., Melvold & Skaugen, 2013). Recently AL, terrestrial LiDAR, and digital photogrammetry data have also been used to investigate possible relations between SD and terrain characteristic (e.g., elevation, slope, aspect, Winstral's wind index, and terrain roughness) (e.g., Grünewald et al., 2010; Helbig et al., 2015; Lehning et al., 2011; Veitinger et al., 2014). Lidar SD data have also been used to verify different snow modeling approaches from the relatively simple statistical model to high-resolution dynamical models (Mott et al., 2010; Trujillo et al., 2007, 2009).

In this study we will use spatially detailed measurements of both SD and the terrain obtained through AL data from Hardangervidda, Southern Norway, to address three important issues for the representation of snow in environmental models. (1) How is the variability of SD related to terrain characteristics, (2) what is an appropriate model for the spatial PDF of SD, and (3) can we parameterize this distribution from available terrain information? The first point will be addressed by correlation analysis between snow and terrain statistics and the second simply by investigating the shape of a large number of empirical distributions of SD. For the third point, which is the main and novel contribution of this study, we will test the model for the spatial variance of SWE presented in Skaugen and Weltzien (2016) for SD data. This approach will take into account the nonlinear relationship between the mean and the standard deviation of SD as observed through the changes in CV through the snow season. This is done by modeling the spatial variance of SD as the sum of variables that are increasingly less correlated as the accumulation proceeds. This will allow for the shape of the spatial PDF of SD to vary through the winter. Parameters of the model will be estimated from measured terrain parameters instead of from observed variability of precipitation which was used for SWE. This represents an extension of the model, since terrain parameters, in principle, are obtainable everywhere, provided there is a sufficiently detailed DTM.

2. Study Area and Data

2.1. Study Area

Hardangervidda is a mountain plateau situated in the eastern part of the western coastal mountain range of Norway (Figure 1). It is one of the largest mountain plateaus in northern Europe and covers an area of about 6,500 km². Most of the plateau is 1,000 m above sea level (m a.s.l.) and hence above the treeline. There are many lakes, streams, and rivers, and most of the plateau is treeless and covered by boulders, gravel, bogs, coarse grasses, mosses, and lichens. The low alpine regions in the northeast and southwest are dominated by grass heaths and dwarf shrub. In the highest part in the west and southwest there is mostly bare rock or lichen/marsh tundra. In the east, at about 1,100 m a.s.l., the landscape is open and flat, whereas in the west and south there are mountain ranges up to 1,700 m a.s.l. In the far northwest, the terrain plunges abruptly down to the fjord Sør fjorden. The western coastal mountain range is a significant orographic feature oriented normally to the prevailing westerly wind flow that dominates the weather in Norway. Moist air masses are lifted by the mountain range and produce an increase in precipitation with elevation on the windward slopes, as well as a decrease on the leeward side of the range and thus on the eastern part of Hardangervidda. Based on the information from *SeNorge.no* (<http://www.SeNorge.no>) the snow accumulation period begins in mid-September in the highest areas, and snowfalls persist throughout the winter months. Maximum snow accumulation is usually in middle to late April, which gives 7 months of snow accumulation. Due to the complex topography of the area and a strong west-east gradient in precipitation, Hardangervidda exhibits large variations in precipitation. Mean annual precipitation varies between 750 and <3,000 mm over a distance of a few tens of kilometers and 50–60% of annual precipitation falls as snow. The weather station at Sandhaug, run by the Norwegian Meteorological Institute, is situated at the middle of one of our 80-km-long lidar flight lines (FLs) at the elevation of 1,250 m a.s.l. (Figure 1). The station provides

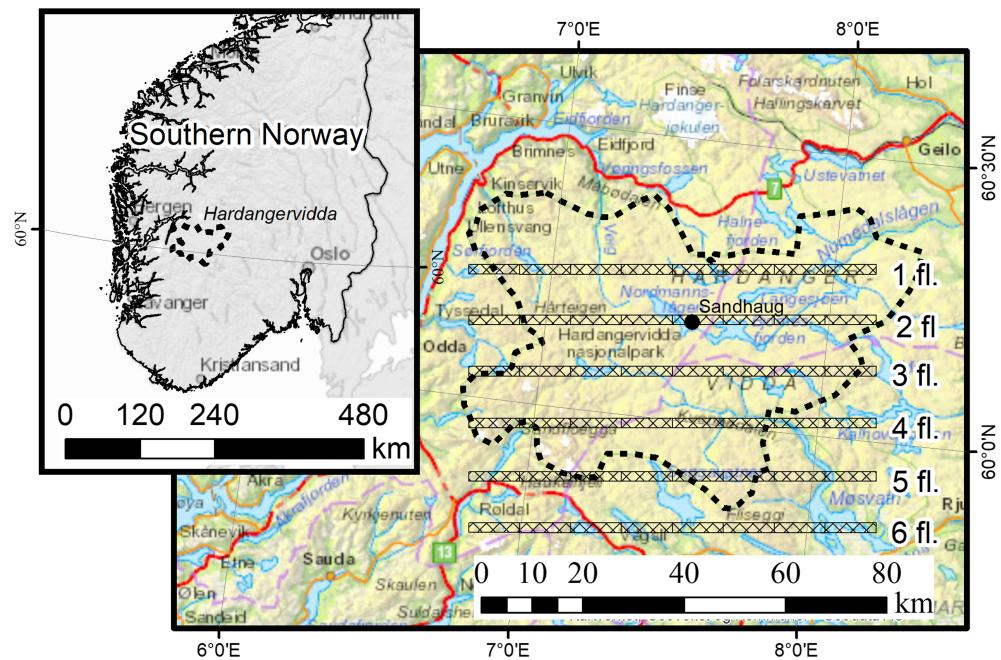


Figure 1. Map of southern Norway and of Hardangervidda showing location of flight lines (fl.), and the Sandhaug meteorological station.

wind measurements needed for estimating the Wind shelter index (Winstral et al., 2002), which is later used as a terrain variable.

2.2. LiDAR Data

In order to study the SD distribution close to snow maximum in spring 2008 and 2009 at Hardangervidda, Melvold and Skaugen (2013) adopted AL altimetry due to its high-resolution and cost-efficient features. The AL data were collected along six 80-km-long FIs following a west-east orientation and have a scanning width of 1,000 m (see Figure 1). The data were collected between 3 and 21 April 2008 (Fls 1–2, 21 April; Fls 3–4, 19 April; and Fls 5–6, 3 April), 21–24 April 2009, and 21 September 2008. The autumn data set represents the minimum snow cover where only perennial snow patches still exist and with leaf-off conditions. In order to reduce slope-induced errors, only a 500-m-wide central part of the swath width was processed. Each FI is separated by 10 km in the north/south direction. In total, the data cover an area of 240-km² sampled in an area of 4,000 km² (80 × 50 km).

Collection, processing, and error estimates of the AL data are presented in detail in Melvold and Skaugen (2013), and only a short summary is given here. The AL data were collected using a Leica ALS50-II instrument with a 1,064-nm wavelength scanning lidar mounted in a fixed-wing aircraft with a flying height above the ground of ~1,800 m. Data were collected at a nominal 1.5 × 1.5-m ground point spacing. The intensity per pulse of the first and last returns was recorded and classified as ground or no ground. The lidar processing was carried out by the lidar contractor (Terratec AS) using a vendor-specific software (TerraScan and TerraPOS).

From the point clouds, winter and summer DTMs were produced from the mean of all the points classified as the ground to a regular grid of 2 × 2 m. The number of original data points per grid cell varied from 0 (in steep slopes and on water bodies) to 9, with an average point density of 3.5. Areas with zero original data points create voids in the DTM, and only the smallest (<40 m²) were interpolated using an interpolation method for hydrologically corrected raster surface based on Hutchinson (1989). Large negative values (defined as <-1 m) and large positive values (defined as >+10) were excluded from the data set. The rest of the negative SDs were set to zero (see Melvold & Skaugen, 2013, for more information). In practice, the data points removed represent <0.01% of the total area sampled and have a negligible influence on SD statistics. All measurements from water bodies (lakes and rivers) were also neglected. In total, we obtained ~8 × 10⁶ SD measurements for each FI, which gives about ~48 × 10⁶ points for each season.

We used the statistical coregistration method described by (Nuth & Kääb, 2011) to avoid having erroneous SD changes from systematic shifts between snow-free and snow-covered DTMs. Melvold and Skaugen (2013) investigated the accuracy of the AL data by comparing AL-derived DTM data with global navigation satellite systems data obtained in spring 2008 along F1 2. They found that the elevation error ranged from -0.95 to $+0.51$ m with a mean error of 0.012 m. The standard error was 0.12 m and very close to the error of 0.11 m as stated by the lidar manufacturer. A more detailed description of errors is found in Melvold and Skaugen (2013).

After the rasterization of the lidar data, the “snow-free” September 2008 DTM was subtracted from the snow surface elevation, the April DTMs, to produce grids of SD.

The development of AL systems in recent years has increased, to some extent, the accuracy of snow data obtained from AL data especially in forested or partly forested areas. The two main reasons are increased sampling density and that the new AL is so-called full-wave-form lidar (see, e.g., Deems et al., 2013, for more information). In open areas with a single return, the benefit of full-wave-form lidar is small compared to the earlier, discrete lidar systems such as the Leica ALS50-II used in this study (Deems et al., 2013; Hancock et al., 2015). More than 90% of Hardangervidda is treeless and thus generally a single-return environment. The forested areas consist of open boreal deciduous forest with birch trees and can, due to leaves-off conditions, also be considered a single-return environment. An examination of the number of returns for each laser pulse shows that 96% of the laser points are classified as first return and ground, so relatively few lidar points are reflections from the canopy. Higher point density of the new AL system will improve the bare-earth and snow-covered grid especially in forested area as the probability of forest canopy penetration increases. Increased sampling density involves less interpolation and thus potentially less errors. This depends, however, on terrain surface complexity, terrain slope, and the chosen grid element size. Brubaker et al. (2013) and Thomas et al. (2017) have shown that a point density of $2\text{--}0.7$ points m^{-2} is sufficient for grid generation at 1- to 2-m resolution and for the calculation of surface roughness parameters. Based on the topography of Hardangervidda, a point density of 0.7 points m^{-2} and a grid resolution 2 m were chosen, which could indicate a slight undersampling. However, based on the error assessments presented in Melvold and Skaugen (2013), the data have provided accurate estimates of SD to the decimeter scale and are hence to be considered of sufficient quality to estimate SD distributions.

3. Methods

3.1. Terrain Parameters

The 2-m-resolution DTM was resampled to 10-m resolution (LasDTM) in order to compare to the national DTM of 10-m resolution. The resampling takes the average of all elevations within the larger cell. This procedure results in a smoothing of the terrain and reduces the amount of data voids.

Based on the new LasDTM we computed several standard terrain parameters. Most terrain variables are local, that is, calculated using the first and second derivatives of the immediate terrain surface. The chosen terrain parameters were elevation, aspect, aspect classes, slope, squared slope, wind shelter index (S_i), and vector roughness measure (VRM).

The standard topographical variables elevation, slope, and aspect were obtained using standard GIS software (ArcGIS software, ESRI). Aspect identifies the slope direction, that is, the downslope direction of the maximum rate of change in value from each cell to its neighbors. We used eight aspect classes: north, northeast, east, southeast, south, southwest, west, and northwest.

Squared slope, $SqS = \tan^2\omega$, where ω is the angle of incline (in radians), represents the rate of maximum change in elevation value from each cell. The mean squared slope in Helbig et al. (2015) expresses the squared ratio between typical height and typical width of topographic features and was used for the same purpose as in this paper.

Wind shelter index (S_i) is a terrain-based upwind/downwind slope predictor developed by Winstral et al. (2002) describing the exposure or shelter to prevailing winds of a location. We used a version of the Winstral algorithm modified by Plattner et al. (2004). S_i was estimated by using the RSAGA package (<https://CRAN.R-project.org/package=RSAGA>) developed in R (www.r-project.org). The S_i has been calculated using the most frequent wind direction (315°) measured at Sandhaug meteorological station (Figure 1)

during the winter periods 2008–2009 and 2009–2010 (not shown) and for a maximum search distance of 100 m and for a chosen width of 30° (15° to each side of the main flow direction).

The VRM has been developed for GIS from a vector approach of Hobson (1972) by Sappington et al. (2010) and is a measure of surface roughness that ranges from 0 (flat) to 1 (most rugged). The VRM was calculated using the `spatialEco` package (<https://CRAN.R-project.org/package=spatialEco>) developed in R (www.r-project.org). We calculated the VRM based on the 10-m surface DTM using a standard 3 × 3 neighborhood. More information about the VRM is found in Sappington et al. (2010).

In addition to the terrain- and the wind-based parameters, also the effect of vegetation has been investigated. The AL data cover areas with low-growing vegetation mostly composed of heather (*Calluna*), sedges, and grasses in the central part of Hardangervidda. In the lower, southern part, the AL data cover areas of open boreal deciduous forest (e.g., Kastdalen & Hjeltnes, 2012). A vegetation/canopy fraction is calculated for each grid cell using the National Land Cover Data AR50 vegetation class (<https://register.geonorge.no/register/versjoner/produktark/norsk-institutt-for-bioekonomi/ar50>). Only grid cells with more than 20% of deciduous forest and/or heather were classified as vegetated. Further stratification of vegetated cells into forest/heather was not carried out due to the low number of vegetated cells.

3.2. Spatial Aggregation of Snow Depth and Terrain Parameters

In Norway, daily maps of interpolated temperature and precipitation on a 1 × 1-km grid have for more than a decade been used by the Norwegian Water Resources and Energy Directorate as the meteorological basis for various operational forecasting services, such as flood, landslide, and avalanche forecasting. In addition, daily maps of various snow parameters are produced based on the gridded meteorological maps (the `seNorge.no` snow model Engeset et al., 2004; Saloranta, 2012, 2016). In order to explain the spatial variability of SD at a scale similar to that of the operational hydrological services, we calculated the statistical moments of SD (mean, standard deviation, skewness, and kurtosis) from the samples of 10 × 10-m SDs for a rectangular grid of 500 × 1,000 m (not 1 × 1 km since the AL data only cover a 500-m-wide transect) and for grid cells with more than 80% (i.e., >~4,000) of valid SD values. The number of grid cells for Fls 1 to 6 are 60 (6 vegetated), 51 (5 vegetated), 45 (4 vegetated), 59 (13 vegetated), 59 (6 vegetated), and 55 (14 vegetated), respectively.

To relate SD to terrain parameters, the corresponding statistical moments were also calculated for each of all the terrain parameters.

3.3. An Analytical Model for the Spatial Frequency Distribution of SD

From the 500 × 1,000-m aggregated data, we investigated which analytical statistical model best suits the empirical distributions of SD. Given the high number of data points (each statistic is estimated from approximately 4,000 values), we have the opportunity to estimate statistical moments of high order with reasonable certainty. A Cullen and Frey graph (Cullen & Frey, 1999) compares the skew and kurtosis of observed data to theoretical values for different statistical models, such as the gamma, the log-normal, and the normal. These three models are typical candidates when an analytical expression for the spatial frequency distribution of snow is needed. In a Cullen and Frey graph, normally distributed values will be located at the point skewness = 0 and kurtosis = 3 (Yevjevich, 1972 p.128).

In addition to the qualitative analysis represented by the Cullen and Frey graph, we subjected the empirical distributions of SD to more classic goodness of fit tests, such as the Anderson-Darling test and the Kolmogorov-Smirnov test (see Delignette-Muller & Dutang, 2015).

3.4. A Model for the Spatial Variance of SD in the Accumulation Season

The dynamic input to a model for the PDF of SD will typically be a mean area value of SD, representing a grid cell, a catchment, or parts of a catchment. We hence need a functional relationship between the mean and the variance of SD in order to estimate the parameters of a (two-parameter) spatial PDF of SD. In addition, one needs to choose an analytical model for the spatial PDF. In Skaugen and Weltzien (2016), the observed relationship between the spatial mean and standard deviation of precipitation was used to formulate such a relationship. It was further noticed that the relationship between the spatial mean and the standard deviation of precipitation was nonlinear in that the rate of increase of the spatial standard deviation deviated from that of the spatial mean. For small values of the spatial mean, the relationship between the mean and the standard deviation was approximately linear, whereas for higher values of the spatial mean, the standard

deviation increased with a smaller rate or not at all. Such a behavior has been observed for measurements of SD and SWE during the accumulation season, where the CV (spatial standard deviation over the spatial mean) decreases as the accumulation seasons proceeds (see Alfnes et al., 2004). Skaugen and Weltzien (2016) presented a model based on the gamma distribution for the spatial variance of SWE in which decreasing temporal correlation is the cause of an attenuating contribution of variance as the accumulation proceeds. This implies that SWE is more evenly distributed in space as the mean SWE increases and that the snow-covered terrain is increasingly smoothed (see also Veitinger et al., 2014). In applying this model for SD, we assume that the observed relationship between the mean and the standard deviation of SWE is similar for SD. Such an assumption is justified if we consider SD as proportional to SWE, that is, $SWE = \beta SD$, where β is the spatially averaged bulk density of snow. Then it can be shown that $E(SWE) = \beta E(SD)$ and $Std(SWE) = \beta Std(SD)$; hence, the relationship observed between the mean and the standard deviation for SWE will be the same, only scaled by β , for SD. Given an input of the spatial mean of SD, the spatial variance, $Var(SD)$, and the spatial mean, $E(SD)$, of the accumulated sum of SD are estimated as follows (from Skaugen & Weltzien, 2016):

$$Var(SD) = E(SD) \frac{1}{\alpha_0} [1 + (n-1)exp(-n/D)] = \frac{\nu}{\alpha^2}, \quad (1)$$

$$E(SD) = n \frac{\nu_0}{\alpha_0} = \frac{\nu}{\alpha} \quad (2)$$

where ν_0 and α_0 are the shape and scale parameters of a gamma-distributed unit SD. In this study we choose the mean value of the unit SD to be 1.0 m, so that $\frac{\nu_0}{\alpha_0} = 1$ and $\nu_0 = \alpha_0$. (Skaugen & Weltzien, 2016, chose the mean value of the unit SWE as 0.1 mm.) n is the number of accumulated unit SD (which in this study will be the number of meters snow at the time of interest), and ν and α are the shape and scale parameters of the gamma-distributed accumulated SD. D is the decorrelation range (in meters of SD), where the exponentially decaying correlation between snowfall units equals $1/e$ (Zawadzki, 1973), $exp(-n/D) = 1/e$. The relationship between the spatial mean and the spatial variance to the parameters of the gamma distribution is as follows:

$$\nu = \frac{E(SD)^2}{Var(SD)} \quad \text{and} \quad \alpha = \frac{E(SD)}{Var(SD)} \quad (3)$$

We intend to test this model for the spatial variance of SD and estimate its parameters (α_0 and D , since ν_0 is determined by the chosen value of the unit snowfall, i.e., $\nu_0/\alpha_0 = 1.0$ m) using terrain information. The parameters α_0 and D are estimated using the nonlinear (weighted) least squares (nls) method provided by R (www.r-project.org). With estimated mean and variance of the distribution, a suitable statistical model (log-normal, gamma, and normal) can be used to represent the spatial PDF of SD in environmental models. See Skaugen and Weltzien (2016) on how equations (1)–(3) were developed for the gamma distribution.

3.5. Exploratory Analysis

In order to investigate possible relationships between the terrain parameters and SD variability, a correlation analysis between snow and terrain statistics and between snow statistics was carried out for the 329 grid cells for each year. The statistics that are correlated are estimated from >4,000 values from 10×10 -m grid-cell values within a $500 \times 1,000$ -m grid cell. The statistics (prefix in brackets) are median (Med), mean (M), standard deviation (Std), skewness (Skw), kurtosis (Kurt), shape parameter of the gamma distribution (ν), scale parameter of the gamma distribution (α), and CV. The analysis was performed for each of the six Fls (45–60 grid cells), for the pooled data of all six Fls (329 grid cells) and for the different landscape classes (LSC1, 281 cells, and LSC2, 48 cells). The Spearman rank correlation method was used since it has no assumption of normally distributed variables.

4. Results

4.1. Correlation Between Snow and Terrain Parameters

At the $500 \times 1,000$ -m scale significant correlations (p value < 0.001) were found between SD and terrain parameters expressing terrain variability (not shown). For both years, high correlations (0.63–0.70) were found between Std_SD and standard deviation of slope, SqS , VRM, and Si . The correlations between the

Table 1
Correlation Between SD and SqS Terrain Statistics for All Flight Lines, 2008 and 2009 for LSC1, Bare Rock.

2008	Med_SqS	M_SqS	Std_SqS	Skw_SqS	Kurt_SqS
Med_SD	0.55	0.56	0.55	0.23	0.23
M_SD	0.60	0.62	0.61	0.24	0.24
Std_SD	0.68	0.70	0.70	0.27	0.27
Kurt_SD	-0.34	-0.33	-0.32		
ν _SD	-0.33	-0.33	-0.31		
CV_SD	0.33	0.36	0.38		
2009	Med_SqS	M_SqS	Std_SqS	Skw_SqS	Kurt_SqS
Med_SD	0.43	0.45	0.45	0.25	0.24
M_SD	0.49	0.51	0.52	0.26	0.26
Std_SD	0.62	0.65	0.66	0.29	0.29
Kurt_SD	-0.21	-0.21	-0.21		
ν _SD	-0.24	-0.25	-0.25	-0.20	
CV_SD	0.36	0.38	0.40		

Note. Prefixes are defined in section 3.4. Only significant (p value < 0.001) correlations are shown. The color shading represents higher/lower correlation.

M_SD and the mean of the terrain parameters SqS and VRM are weaker (0.60–0.61). The other terrain parameters (aspect, elevation, and aspect classes) showed no significance or weaker correlations.

The correlations between the terrain parameters are high. For example, the standard deviation of SqS is correlated to the standard deviation of VRM, Si, and elevation with 0.91, 0.90, and 0.79, respectively. This suggests that only one of the parameters should be used since little new information is obtained by including additional terrain parameters. Although VRM has a slightly higher correlation with Std_SD than SqS (0.70 vs. 0.69 in 2008 and 0.64 vs. 0.63 in 2009), SqS is chosen as the terrain parameter for this study since SqS is simpler to calculate than VRM and is independent of wind data (unlike Si).

4.2. Correlation Analysis for the Statistical Moments of Snow Depth and Squared Slope

From the findings in the previous section, we further investigated the relationship between snow and the terrain parameter SqS. In addition, we investigated whether it would be relevant to stratify the SD statistics according to landscape classes (LSC). When pooling all grid cells for the six Fls together for the 2009 data, we could see that the snow statistics (M_SD and Std_SD) were significantly correlated (p value < 0.001) to LSC with correlations equal to 0.37 and 0.52, respectively (not shown).

Based on this finding, we continue the correlation analysis for separate LSC.

The results of the correlation analysis between SD and SqS statistics for LSC1 are shown in Table 1. As very few data points (48 grid cells) describe the snow/terrain statistics for forest/wetlands (LSC2), few correlations were found significantly different from zero and are not shown. Correlations for snow statistics are shown in Table 2 for the two different LSC.

From Table 1, we note that especially M_SD and Std_SD are well correlated with M_SqS and Std_SqS. The higher statistical moments for SD, such as the skewness and kurtosis, are not significantly, or very weakly, correlated with SqS. On the other hand, Table 2, upper triangle (LSC1), shows how the mean M_SD is highly correlated to the higher moments of SD (variance, skewness, and kurtosis). In addition, we see that the shape (ν _SD) and scale (α _SD) of the gamma distribution are highly correlated to the mean SD. In the lower triangle (LSC2), we find that the M_SD is correlated to Std_SD, but not to the higher statistical moments of SD.

4.3. Choosing a Statistical Distribution for the Spatial PDF of Snow Depth

Figure 2 shows how the skewness and kurtosis estimated from 329 empirical distributions (both LSC are included) of SD for the years 2008 (a) and 2009 (b), compared to the theoretical values of the normal, log-normal, and gamma distribution. The colors represent how the mean SD of each distribution compares to the highest mean SD for each year. Blue indicates means close to the maximum; green and finally red indicate means smaller than the maximum. There is a substantial scatter for both years, but especially for 2009, the gamma distribution seems to be the best suited. In addition, we can note that as the mean increases (the color trends toward blue), the skew decreases (points to the left), indicating that the individual distribution changes shape as a function of the mean, which is consistent with the high correlations found between M_SD and the higher-order moments of SD, ν _SD, and α _SD for LSC1 in Table 2.

All empirical distributions were subjected to goodness of fit tests (see Delignette-Muller & Dutang, 2015) such as the Anderson-Darling test and the Kolmogorov-Smirnov test. Using the Anderson-Darling test, 68% were best approximated using the gamma distribution, 14% the log-normal, and 18% the normal distribution. When testing the distributions for the individual LSC, the partition became 68%, 14% and 18% for LSC1, and 70%, 17%, and 13% for LSC2. Similar results were obtained using the Kolmogorov-Smirnov test.

4.4. Estimating Parameters for the Spatial Variance Model of SD

The correlation analysis above has shown that parameters describing the variability of the terrain are highly correlated to the variability of snow for the bare rock class (LSC1). We have also seen that the Std_SD is

Table 2
Correlation Between Snow Statistics for All Flight Lines for 2008 and 2009.

2008	Med_SD	M_SD	Std_SD	Skw_SD	Kurt_SD	ν _SD	α _SD	CV_SD
Med_SD	1	0.99	0.81	-0.68	-0.70	-0.83	0.66	
M_SD	0.99	1	0.88	-0.62	-0.69	-0.78	0.60	
Std_SD	0.40	0.46	1	-0.38	-0.63	-0.56	0.37	0.45
Skw_SD				1	0.87	0.95	-0.99	0.44
Kurt_SD				0.66	1	0.88	-0.86	
Sh_SD	-0.47	-0.43		0.97	0.66	1	-0.96	0.32
Sc_SD				-0.99	-0.69	-0.98	1	-0.42
CV_SD			0.76					1
2009	Med_SD	M_SD	Std_SD	Skw_SD	Kurt_SD	ν _SD	α _SD	CV_SD
Med_SD	1	0.98	0.81	-0.69	-0.71	-0.85	0.69	
M_SD	0.99	1	0.89	-0.61	-0.68	-0.80	0.61	
Std_SD		0.55	1	-0.38	-0.57	-0.59	0.38	0.42
Skw_SD				1	0.92	0.96	-1	0.47
Kurt_SD				0.83	1	0.92	-0.92	0.18
ν _SD	-0.53			0.98	0.83	1	-0.96	0.34
α _SD				-1	-0.84	-0.98	1	-0.47
CV_SD			0.73			0.58	-0.60	1

Note. Correlations for LSC1, bare rock is in the upper triangle, and correlations for LSC2, wetlands/forest is in the lower triangle (in italics). Only significant (p value < 0.001) correlations are shown. The color shading represents higher/lower correlation.

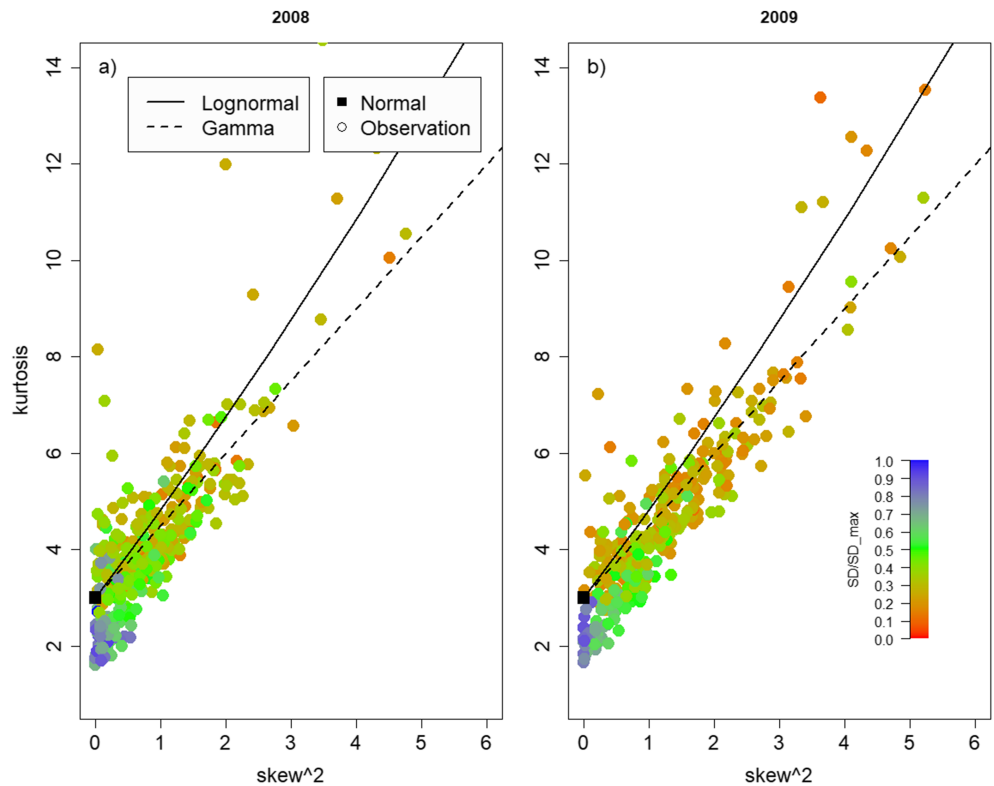


Figure 2. Cullen and Frey graphs of the skew and kurtosis of 658 empirical distributions for 500 × 1,000-m grid cells at Hardangervidda for 2008 (a) and 2009 (b) compared to the theoretical values of the gamma, log-normal, and normal (skewness = 0 and kurtosis = 3) distribution. Blue color indicates mean values close to the maximum mean, and green to finally red indicate mean values smaller than the maximum mean.

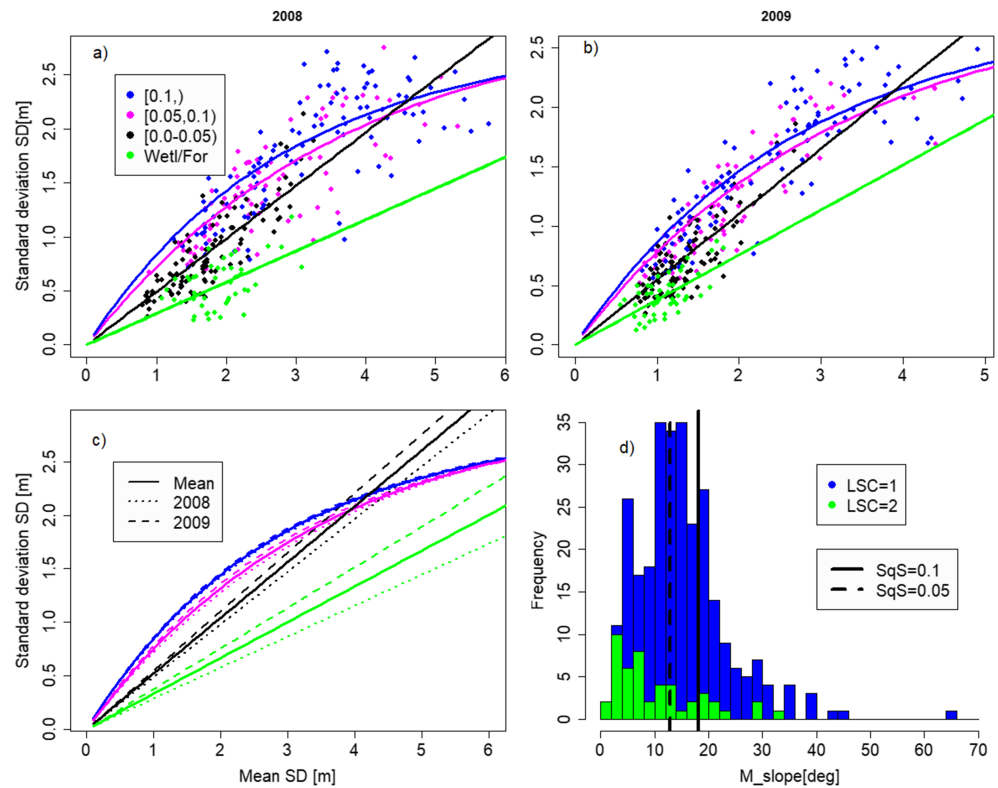


Figure 3. Model of the spatial variability of SD fitted to the 2008 (a) and 2009 (b) AL data. The mean model is in panel (c). The colors indicate model and observations for different classes of squared slope and landscapes. Blue, $\text{Std_SqS} \geq 0.1$; magenta, $0.05 \leq \text{Std_SqS} < 0.1$; black, $0.0 < \text{Std_SqS} < 0.05$; and green, wetlands and forest (LSC2). All units are in meters. Panel (d) shows the histograms of slopes for LSC1 and LSC2, with $\text{SqS} = 0.1$ and 0.05 indicated with vertical lines.

highly correlated to M_SD . Hence, we conclude that the Std_SD is a function of M_SD , a dynamic variable, and the spatial variability of the terrain, a static variable. In addition, Figure 3 shows that the relationship between M_SD and Std_SD often is nonlinear, which, for SWE in Skaugen and Weltzien (2016), was explained by the decreasing correlation between the accumulated snowfall units. Figure 3 also shows the model (equation (1)) with model parameters estimated using nonlinear and linear least square methods for the Hardangervidda data for 2008 and 2009. The models are fitted to different classes of Std_SqS for LSC1 ($0.0 \leq \text{Std_SqS} < 0.05$, $0.05 \leq \text{Std_SqS} < 0.1$, and $\text{Std_SqS} \geq 0.1$) and to the landscape class LSC2, wetland/forest. At Hardangervidda, the LSC2 area is typically smooth and hence with a low Std_SqS (see Figure 3d) where histograms of the slopes for LSC1 and LSC2 are shown. It is therefore not possible to differentiate with respect to Std_SqS for LSC2. The thresholds for Std_SqS were decided from a qualitative assessment that appeared consistent for both 2008 and 2009. Table 3 shows the estimated parameters of the model, the scale parameter of the unit snowfall α_0 , and the decorrelations range D (measured in meters of snow). Nonlinear functions were fitted to the LSC1 and for Std_SqS greater than 0.05. For $\text{Std_SqS} < 0.05$ and for LSC2, it was only possible to fit linear functions. The snow variability for the 2 years shows very similar behavior.

4.5. Model Validation

In Figures 4a and 4b we resampled 230 (70%) of the data points 32 times and estimated the model parameters for each sample. The models were then validated predicting Std_SD for the opposite year. Correlation (Cor), bias, and explained variance (ExplVar) are hence estimated from $\sim 10,000$ points. In Figure 4c we used 230 data points (70%) from each year to estimate parameters of the mean model 51 times. The models were validated predicting Std_SD for the points not used to estimate model parameters ($\sim 10,000$ points). Figure 4d shows how the model could be applied for catchment-scale information of terrain and LSC. The SD and SqS statistics were estimated for 48 aggregated grids of size 5.1 km^2 ($500 \text{ m} \times 10.25 \text{ km}$), which is closer to

Table 3
Parameters of Std_SD Model 2008 and 2009 and Mean Model for Different Std_SqS Values and for LSC1 and LSC2

Std_SqS	α_0	D	Regression type
2008			
>0.1	1.43	2.56	Nonlinear
0.05–0.1	1.92	3.64	Nonlinear
0.0–0.05	0.49		Linear
Wtl/Forest	0.29		Linear
2009			
>0.1	1.34	2.4	Nonlinear
0.05–0.1	1.63	3.01	Nonlinear
0.0–0.05	0.55		Linear
Wtl/Forest	0.38		Linear
Mean model			
>0.1	1.39	2.48	Nonlinear
0.05–0.1	1.78	3.32	Nonlinear
0.0–0.05	0.52		Linear
Wtl/Forest	0.33		Linear

the scale of a catchment or elevation bands in a semidistributed hydrological model. The same bootstrapping procedure as above was used, and the models were validated predicting Std_SD for the points not used to estimate model parameters (~6,000 points). The explained variance of the mean model for the scale of 5.1 km² is equal to that of 0.5 km².

Table 2 shows very high correlations between the M_SD and the Std_SD with 0.88 and 0.89 respectively for the years 2008 and 2009. It is therefore instructive to investigate if such a linear relationship between the standard deviation and the spatial mean can be an alternative or even a better model. Such a linear model is equivalent to assuming a constant CV of SD similar to the model in Pomeroy et al. (2004). Figure 5a shows the result of a model where the spatial standard deviation of SD is a linear function of the spatial mean. A similar bootstrapping procedure as in Figure 4c was applied. We also investigated how the parameterization of Helbig et al. (2015) compared with our model. We calculated the topographic parameters needed for the Helbig et al. (2015) expression for the standard deviation of SD from our LasDTM for each grid cell of 500 × 1,000 m and bootstrapped the calibration parameters as above. Figure 5b shows

the results and that the explained variance (ExplVar) for the Helbig et al. (2015) parameterization is higher than for the model that assumes constant CV, but lower than for the model proposed in this study.

In Figures 4 and 5, points from each Fl from LSC1 have different colors. In the effectively 4,000-km²-large area, no apparent spatial biases in the north (Fl 1)-south (Fl 6) direction can be seen.

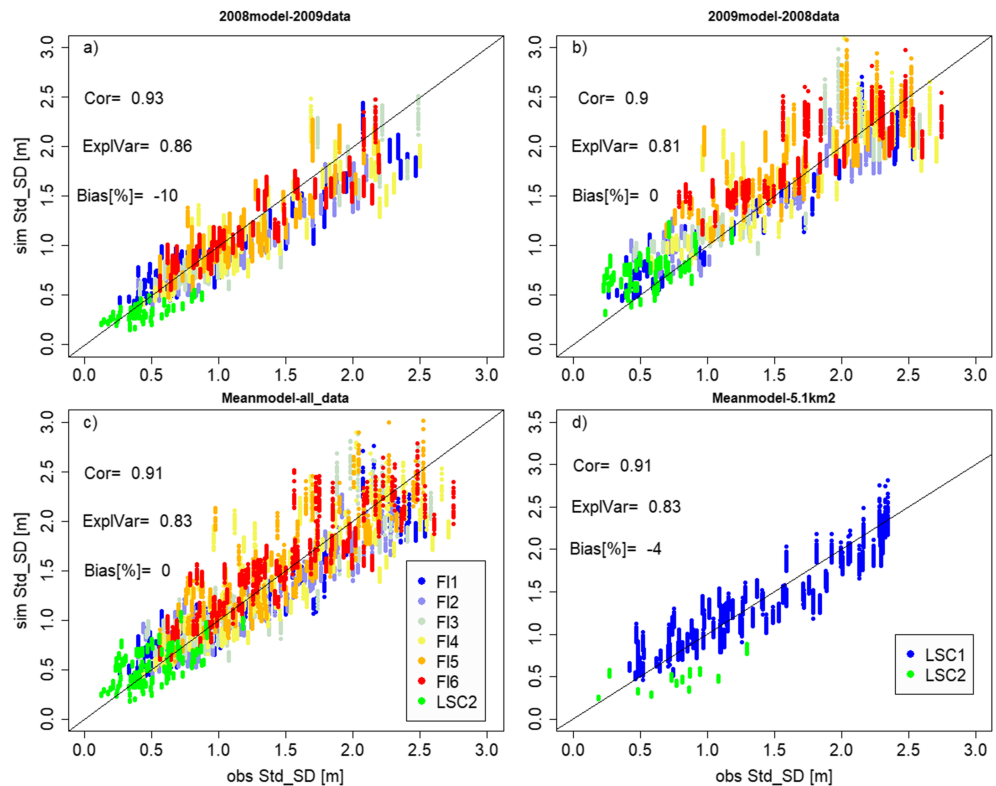


Figure 4. Observed standard deviation of SD versus bootstrapped simulated values using 70% of data. Colored circles indicate different flight lines as shown in legend. Green circles represent LSC2. (a) Model based on 2008 data validated on 2009 data. (b) Model based on 2009 data validated on 2008 data. (c) Mean model validated on 30% of 2008–2009 data. (d) Mean model for 5.1 km² validated on 30% of 2008–2009 data.

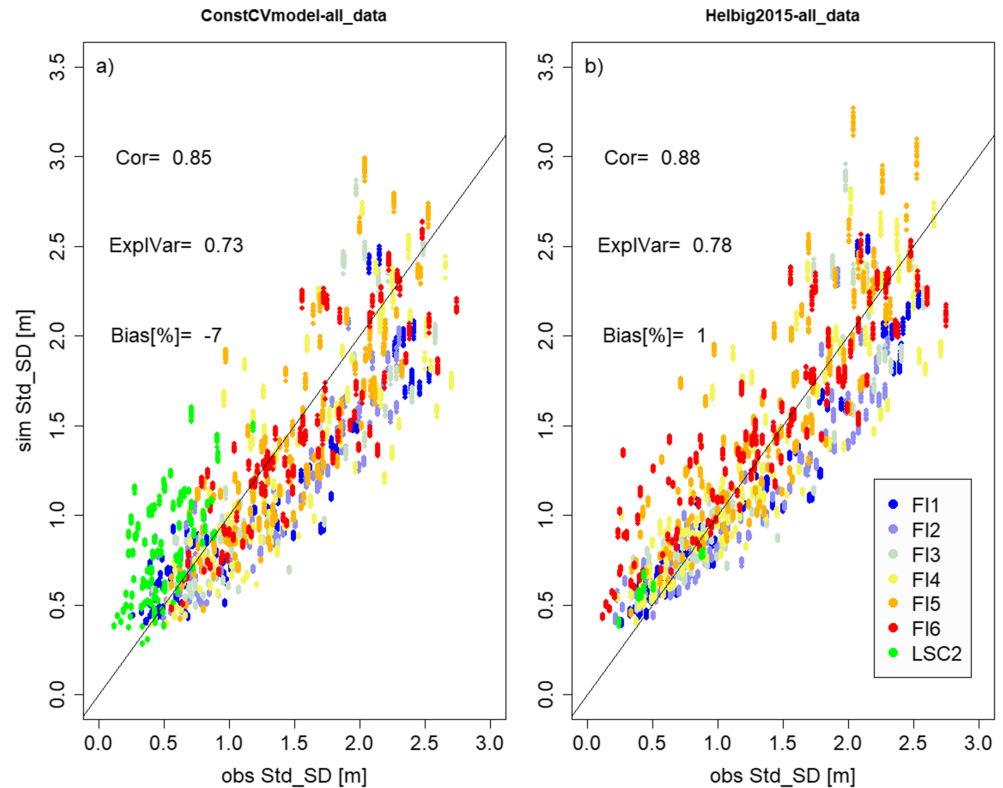


Figure 5. Observed standard deviation of SD versus bootstrapped simulated values using 70% of data. (a) Constant CV model and (b) the parameterization of Helbig et al. (2015). Colored circles indicate different flight lines as shown in legend. Green circles represent LSC2.

5. Discussion

It has been a longstanding ambition to model snow variables from topographical and vegetation characteristics of the landscape. Many studies report quite modest correlations between snow and these characteristics (Gisnås et al., 2016; Jost et al., 2007; Lehning et al., 2011), and furthermore, these correlations are dependent on the spatial support of the dependent variable and the independent variables (Erxleben et al., 2002; Jost et al., 2007). For the applied scale in this study, 0.5 km^2 , we find significant correlations between snow statistics, such as the mean and the standard deviation of SD and the statistics (mean and standard deviation) of the terrain parameter Sqs calculated from the $10 \times 10\text{-m}$ grid cell values comprised by the 0.5-km^2 grid. In addition, we find significant correlations to LSC when we stratify the data into bare rock (LSC1) and wetland/forest (LSC2). Gisnås et al. (2016) and Lehning et al. (2011) also found high correlations in Norway and Switzerland, respectively, when relating SD variability to various roughness indexes for alpine areas. It is noticeable that including information of wind (i.e., using the Winstal index S_i) does not lead to increased correlations between terrain and of SD at the scales used in this study. Several authors discuss the dominant processes for shaping the distributions of SD at different scales (Clark et al., 2011; Liston, 2004). At the scales used in this study ($\geq 0.5 \text{ km}^2$), orographic precipitation is suggested as the dominant process. One might argue that topography also shapes the near-surface wind fields, which also influences the snow deposition (Lehning et al., 2008; Mott et al., 2011), so perhaps, at scales $\geq 0.5 \text{ km}^2$, the wind effect of wind is already captured when using terrain as a predictor for snow distribution. Especially for LSC1, the correlations between the M_{SD} and Std_{SD} are high. Pomeroy et al. (2004) found similar correlations for various landscape types in Canada, and a constant CV model (see section 4.5) may be justified. It is interesting to note, however, that M_{SD} is also highly correlated to the skewness and kurtosis of SD (and the ν and α parameters of the gamma distribution), statistics that measure the shape of the distribution (see Table 2 and also Figure 2). We can also note (from Table 1) that SqS is less influential for the skewness and kurtosis of SD. These findings suggest that the shape

of the distribution of SD during the accumulation season is dynamic (since M_{SD} changes) and more influenced by the amount of snow than the terrain.

The Cullen and Frey graphs (Figures 2a–2b in Cullen & Frey, 1999) show that the normal, the log-normal, and the gamma distribution may, for individual snow courses, all be reasonable choices for the spatial frequency distribution of snow. The goodness of fit tests, however, favor the gamma distribution for 68% of the empirical distributions. In addition to being the best fit to the empirical distributions, the gamma distribution has attractive mathematical features, which have been used to model spatial distribution of SWE in hydrological models (Skaugen, 2007; Skaugen & Randen, 2013; Skaugen & Weltzien, 2016). In such a model, the spatial distribution of SWE is dynamic, that is, its shape evolves from skewed at the beginning of the accumulation season, to a more symmetrical distribution as the accumulation proceeds and to a more skewed again as the snow melts. This pattern has been observed for measured spatial distributions of SD and SWE (see Alfnes et al., 2004; Skaugen, 2007) and partly for SD in this study (see Figure 2 and the correlations in Table 2).

The abundance of data presented in this study confirms and clearly illustrates the nonlinear relationship between the spatial mean and standard deviation of SD (see Figure 3). Although a linear approach seems appropriate for small and medium mean SDs (<2–3 m), we can see, in Figure 3, that the rate of increase for the standard deviation decreases as the mean increases. The presented model captures the nonlinear relationship by introducing correlation (equation (1)) and by stratifying the model according to squared slope and LSC. The results for estimating the spatial variability of SD, shown in Figure 4 with explained variance for spatial scales of 0.5 and 5.1 km² ranging from 81–83%, compare favorably with the alternative parameterizations of constant CV and that of Helbig et al. (2015) shown in Figure 5. The model of Helbig et al. (2015) has strong similarities to our model since it includes topography (which is parameterized including squared slope) and the mean SD and has a CV that decreases as the mean increases. The influence of topography is represented by a constant. A difference between the models is that in our model, the effect of the topography is dynamic, that is, as the SD increases, the significance of correlation and its variance contribution decreases (see equation (1), where the last term [the correlation] decreases as n increases). The distribution of SD hence evolves toward a more symmetrical distribution, which is consistent with the observations shown in Figure 2. The study of Helbig et al. (2015) predicted the standard deviation of SD for scales increasing from 0.0025 to 9 km² with an overall explained variance of 45%. The results in Figure 4 also compare well to other previous studies on spatial variance of SD. In Grünewald et al. (2013), the spatial variability of SD at mountainous sites across the world was modeled locally with multiple regression at a scale of 0.16 km² with explained variance of 30% to 91%. A global model, however, only achieved 23% explained variance. López-Moreno et al. (2015) found that multiple regression model for predicting the variance of SD explained 50% at 25 × 25-m scale and 70% at the 0.01-km² scale. Common to the models in Helbig et al. (2015), López-Moreno et al. (2015), and Grünewald et al. (2013) is that increasing the spatial scales increases the explained variance. In our study, however, the explained variances for 0.5 and 5.1 km² are equal (see Figures 4c and 4d).

The model presented here appears to work well for the study area using observed terrain variability and observed mean SD. In operational hydrology, however, we would have to rely on modeled mean SD either from interpolated meteorological grids or numerical weather prediction models using estimated snow bulk density. Such procedures obviously introduce uncertainty through model structures and calibrated parameters. The SeNorge snow model (Saloranta, 2012) has, since 2004, estimated SWE, SD, and hence snow density for all of Norway on a 1 × 1-km² grid at a daily basis with acceptable results (see Skaugen et al., 2018). The model presented here can be used to validate the spatial properties of SD in such models and form the basis for parameterizing the spatial variability of SWE in hydrological models.

Although the results are presented for data acquired at a time of (the assumed) “peak accumulation,” the model performs well over a range of mean SD values. This suggests that the model can be used to estimate the spatial variance of SD at any time during the accumulation season. In the melt season, however, Egli and Jonas (2009) demonstrate hysteresis effects between the mean and standard deviation of SD, so the functional relationship between the mean and standard deviation found for the accumulation season may no longer apply. The model appears to work well for both LSC and with no apparent north-south biases. The model needs, however, to be further validated for different regions.

6. Conclusions

When snow and terrain parameters were aggregated to $500 \times 1,000$ m, we found that the standard deviation of several terrain parameters is highly correlated with the standard deviation of SD. The terrain parameters, and the squared slope in particular, explain large parts of the spatial variance of snow. In addition, the spatial standard deviation of SD was significantly correlated to LSC (bare rock and wetland/forest) and to the mean spatial SD. The mean spatial SD was also highly correlated to the skew and kurtosis of SD, indicating that the shape of the distribution of SD is dynamic, that it evolves as accumulation proceeds. The collection of terrain parameters investigated in this study was highly correlated, suggesting that little additional information is gained by including more than one terrain parameter.

In order to establish which analytical statistical distribution best represents the SD distribution at Hardangervidda, we visually inspected the Cullen and Frey graphs of 658 empirical distributions, of which each consisted of approximately 4,000 SDs sampled from the 0.5-km^2 grid cells. The Cullen and Frey graphs show that gamma, log-normal, and normal all can be suitable choices of PDF, but by the Anderson-Darlington test and Kolmogorov-Smirnov test, the gamma distribution emerged as the most suitable distribution for 68% of the distributions, 14% the log-normal, and 18% the normal. The Cullen and Frey graphs also show how the skew and kurtosis of the distribution of SD decrease as the M_{SD} increases.

A model for the spatial standard deviation of SD is proposed that combines the mean SD, the terrain parameter SqS , and the LSC to determine the variance of SD. When validated, the model explained 81–83% of the observed variability of SD for the spatial scales of 0.5 and 5.1 km^2 . We have chosen the gamma distribution to approximate the shape of the spatial frequency distribution of SD, and the model provides the mean and variance of SD so that the parameters of the gamma distribution can be estimated. The gamma distribution can hence serve as a model for SD in environmental models. This exercise needs to be repeated for AL data from a different region (or a country) so that the possible generality of the method can be verified.

Acknowledgments

We would like to thank T. Saloranta at NVE, Nora Helbig, and an anonymous reviewer for constructive and thoughtful comments, improving the paper. This paper is a deliverable in the SnowHow project (244153/E10) financed by Norwegian Research Council, Glommen and Laagen Brukseierforening, E-CO, Trøndelag Energiverk, and HYDRO Energi. In addition, research done within NVE's FoU-project 80208 has also contributed to this study. Their support is gratefully acknowledged. The Lidar data used in this study are available online (<https://doi.org/10.5281/zenodo.2572732>).

References

- Alfnes, E., Andreassen, L. M., Engeset, R. V., Skaugen, T., & Udnaes, H. C. (2004). Temporal variability in snow distribution. *Annals of Glaciology*, *38*, 101–105.
- Anderton, S. P., White, S. M., & Alvera, B. (2004). Evaluation of spatial variability in snow water equivalent for a high mountain catchment. *Hydrological Processes*, *18*(3), 435–453.
- Blöschl, G. (1999). Scaling issues in snow hydrology. *Hydrological Processes*, *13*(14–15), 2149–2175.
- Brubaker, K. M., Myers, W. L., Drohan, P. J., Miller, D. A., & Boyer, E. W. (2013). The use of LiDAR terrain data in characterizing surface roughness and microtopography. *Applied and Environmental Soil Science*, *2013*, 13.
- Brun, E., David, P., Sudul, M., & Brunot, G. (1992). A numerical model to simulate snow-cover stratigraphy for operational avalanche forecasting. *J Glaciol*, *38*(128), 13–22.
- Buttle, J. M., & McDonnell, J. J. (1987). Modelling the areal depletion of snowcover in a forested catchment. *Journal of Hydrology*, *90*(1), 43–60.
- Clark, M. P., Hendrikx, J., Slater, A. G., Kavetski, D., Anderson, B., Cullen, N. J., et al. (2011). Representing spatial variability of snow water equivalent in hydrologic and land-surface models: A review. *Water Resources Research*, *47*, W07539. <https://doi.org/10.1029/2011WR010745>
- Cullen, A. C., & Frey, H. C. (1999). *Probabilistic techniques in exposure assessment. a handbook for dealing with variability and uncertainty in models and inputs*. Plenum Press, New York and London.
- Deems, J. S., Fassnacht, S. R., & Elder, K. J. (2006). Fractal distribution of snow depth from lidar data. *Journal of Hydrometeorology*, *7*(2), 285–297.
- Deems, J. S., Painter, T. H., & Finnegan, D. C. (2013). Lidar measurement of snow depth: A review. *J Glaciol*, *59*(215), 467–479.
- Delignette-Muller, M. L., & Dutang, C. (2015). fitdistrplus. *An R Package for Fitting Distributions*, *J Stat Softw*, *64*(4), 1–34.
- Donald, J. R., Soulis, E. D., Kouwen, N., & Pietroniro, A. (1995). A Land Cover-Based Snow Cover Representation for Distributed Hydrologic Models. *Water Resources Research*, *31*(4), 995–1009.
- Egli, L., Griessinger, N., & Jonas, T. (2011). Seasonal development of spatial snow-depth variability across different scales in the Swiss Alps. *Annals of Glaciology*, *52*(58), 216–222.
- Egli, L., & Jonas, T. (2009). Hysteretic dynamics of seasonal snow depth distribution in the Swiss Alps. *Geophysical Research Letters*, *36*, L02501. <https://doi.org/10.1029/2008GL035545>
- Elder, K., Cline, D., Liston, G. E., & Armstrong, R. (2009). NASA Cold Land Processes Experiment (CLPX 2002/03): Field measurements of snowpack properties and soil moisture. *Journal of Hydrometeorology*, *10*(1), 320–329.
- Elder, K., Dozier, J., & Michaelsen, J. (1991). Snow accumulation and distribution in an alpine watershed. *Water Resources Research*, *27*(7), 1541–1552.
- Engeset, V. R., Tveito, O. E., Alfnes, E., Mengistu, Z., Udnaes, H.-C., Isaksen, K., & Førland, E. J. (2004). *Snow map system for Norway, paper presented at XXIII Nordic Hydrological Conference, 8–12 August 2004, NHP report 48*. Estonia: Tallinn.
- Erickson, T. A., Williams, M. W., & Winstral, A. (2005). Persistence of topographic controls on the spatial distribution of snow in rugged mountain terrain, Colorado, United States. *Water Resources Research*, *41*, W04014. <https://doi.org/10.1029/2003WR002973>
- Erxleben, J., Elder, K., & Davis, R. (2002). Comparison of spatial interpolation methods for estimating snow distribution in the Colorado Rocky Mountains. *Hydrological Processes*, *16*(18), 3627–3649.

- Essery, R., & Pomeroy, J. (2004). Vegetation and topographic control of wind-blown snow distributions in distributed and aggregated simulations for an Arctic tundra basin. *Journal of Hydrometeorology*, 5(5), 735–744.
- Gisnås, K., Westermann, S., Schuler, T. V., Melvold, K., & Eitzmuller, B. (2016). Small-scale variation of snow in a regional permafrost model. *Cryosphere*, 10(3), 1201–1215.
- Grünwald, T., Schirmer, M., Mott, R., & Lehning, M. (2010). Spatial and temporal variability of snow depth and ablation rates in a small mountain catchment. *Cryosphere*, 4(2), 215–225.
- Grünwald, T., Stotter, J., Pomeroy, J. W., Dadic, R., Banos, I. M., Marturia, J., et al. (2013). Statistical modelling of the snow depth distribution in open alpine terrain. *Hydrology and Earth System Sciences*, 17(8), 3005–3021.
- Hancock, S., et al. (2015). Waveform lidar over vegetation: An evaluation of inversion methods for estimating return energy. *Remote Sens Environ*, 164, 208–224.
- Helbig, N., van Herwijnen, A., Magnusson, J., & Jonas, T. (2015). Fractional snow-covered area parameterization over complex topography. *Hydrology and Earth System Sciences*, 19(3), 1339–1351.
- Hiemstra, C. A., Liston, G. E., & Reiners, W. A. (2002). Snow redistribution by wind and interactions with vegetation at upper treeline in the Medicine Bow Mountains. *Wyoming, USA, Arct Antarct Alp Res*, 34, 262–273.
- Hobson, C. G. (1972). Surface roughness in topography: Quantitative approach. In R. J. Chorley (Ed.), *Spatial analysis in geomorphology* (pp. 221–245). New York, New York, USA: Haper and Row.
- Hopkinson, C., Sitar, M., Chasmer, L., & Treitz, P. (2004). Mapping snowpack depth beneath forest canopies using airborne lidar. *Photogrammetric Engineering and Remote Sensing*, 70(3), 323–330.
- Hutchinson, M. F. (1989). A new procedure of gridding elevation and stream line data with automatic removal of spurious pits. *Journal of Hydrology*, 106, 211–232.
- Jost, G., Weiler, M., Gluns, D. R., & Alila, Y. (2007). The influence of forest and topography on snow accumulation and melt at the watershed-scale. *Journal of Hydrology*, 347(1-2), 101–115.
- Kastdalen, L., & Hjeltnes, A. W. (2012). Vegetasjonskartlegging med satellittdata Optimalisering av analysemetodikk (in Norwegian), *HIT skrift nr. In 7/2012*. Telemark: University College, Bø, 1–66.
- Kolberg, S., & Gottschalk, L. (2010). Interannual stability of grid cell snow depletion curves as estimated from MODIS images. *Water Resources Research*, 46. W11555. <https://doi.org/10.1029/2008WR007617>
- Kuchment, L. S., & Gelfan, A. N. (1996). The determination of the snowmelt rate and the meltwater outflow from a snowpack for modelling river runoff generation. *Journal of Hydrology*, 179(1), 23–36.
- Lehning, M., Grünwald, T., & Schirmer, M. (2011). Mountain snow distribution governed by an altitudinal gradient and terrain roughness. *Geophysical Research Letters*, 38, L19504. <https://doi.org/10.1029/2011GL048927>
- Lehning, M., Lowe, H., Rysler, M., & Raderschall, N. (2008). Inhomogeneous precipitation distribution and snow transport in steep terrain. *Water Resources Research*, 44. W07404. <https://doi.org/10.1029/2007WR006545>
- Liston, G. E. (2004). Representing subgrid snow cover heterogeneities in regional and global models. *Journal of Climate*, 17(6), 1381–1397.
- Liston, G. E., & Elder, K. (2006). A distributed snow-evolution modeling system (SnowModel). *Journal of Hydrometeorology*, 7(6), 1259–1276.
- Liston, G. E., Haehnel, R. B., Sturm, M., Hiemstra, C. A., Berezovskaya, S., & Tabler, R. D. (2007). Instruments and methods simulating complex snow distributions in windy environments using SnowTran-3D. *J Glaciol*, 53(181), 241–256.
- Liston, G. E., Pielke, R. A., & Greene, E. M. (1999). Improving first-order snow-related deficiencies in a regional climate model. *Journal of Geophysical Research*, 104(D16), 19,559–19,567.
- Liston, G. E., & Sturm, M. (2002). Winter precipitation patterns in arctic Alaska determined from a blowing-snow model and snow-depth observations. *Journal of Hydrometeorology*, 3, 646–659.
- López-Moreno, J. I., Revuelto, J., Fassnacht, S. R., Azorín-Molina, C., Vicente-Serrano, S. M., Morán-Tejeda, E., & Sexstone, G. A. (2015). Snowpack variability across various spatio-temporal resolutions. *Hydrological Processes*, 29(6), 1213–1224.
- Luce, C. H., & Tarboton, D. G. (2004). The application of depletion curves for parameterization of subgrid variability of snow. *Hydrological Processes*, 18(8), 1409–1422.
- Luce, C. H., Tarboton, D. G., & Cooley, K. R. (1999). Sub-grid parameterization of snow distribution for an energy and mass balance snow cover model. *Hydrological Processes*, 13(13), 1921–1933.
- Marchand, W. D., & Killingtveit, A. (2004). Statistical properties of spatial snowcover in mountainous catchments in Norway. *Nord Hydrol*, 35(2), 101–117.
- Marchand, W. D., & Killingtveit, A. (2005). Statistical probability distribution of snow depth at the model sub-grid cell spatial scale. *Hydrological Processes*, 19(2), 355–369.
- Melvold, K., & Skaugen, T. (2013). Multiscale spatial variability of lidar-derived and modeled snow depth on Hardangervidda, Norway. *Annals of Glaciology*, 54(62), 273–281.
- Mott, R., Egli, L., Grünwald, T., Dawes, N., Manes, C., Bavay, M., & Lehning, M. (2011). Micrometeorological processes driving snow ablation in an Alpine catchment. *Cryosphere*, 5(4), 1083–1098.
- Mott, R., Schirmer, M., Bavay, M., Grünwald, T., & Lehning, M. (2010). Understanding snow-transport processes shaping the mountain snow-cover. *Cryosphere*, 4(4), 545–559.
- Nuth, C., & Kääb, A. (2011). Co-registration and bias corrections of satellite elevation data sets for quantifying glacier thickness change. *Cryosphere*, 5(1), 271–290.
- Plattner, C., Braun, L. N., & Brenning, A. (2004). The spatial variability of snow accumulation on Vernagtferner, Austrian Alps, in Winter 2003/2004. *Zeitschrift für Gletscherkunde und Glazialgeologie*, 39, 43–57.
- Pomeroy, J., Essery, R., & Toth, B. (2004). Implications of spatial distributions of snow mass and melt rate for snow-cover depletion: Observations in a subarctic mountain catchment. *Annals of Glaciology*, 38, 195–201.
- Sæthun, N. R. (1996). The “Nordic” HBV model *Publication nr. 7*. Norwegian Energy and Water Resources Administration, Oslo.
- Saloranta, T. M. (2012). Simulating snow maps for Norway: Description and statistical evaluation of the seNorge snow model. *Cryosphere*, 6(6), 1323–1337.
- Saloranta, T. M. (2016). Operational snow mapping with simplified data assimilation using the seNorge snow model. *Journal of Hydrology*, 538, 314–325.
- Sappington, J. M., Longshore, K. M., & Thompson, D. B. (2010). Quantifying Landscape Ruggedness for Animal Habitat Analysis: A case study using Bighorn Sheep in the Mojave Desert. *The Journal of Wildlife Management*, 71(5), 1419–1426.
- Schirmer, M., Wirz, V., Clifton, A., & Lehning, M. (2011). Persistence in intra-annual snow depth distribution: 1. *Measurements and topographic control*, *Water Resources Research*, 47, W09516.

- Skaugen, T. (2007). Modelling the spatial variability of snow water equivalent at the catchment scale. *Hydrology and Earth System Sciences*, 11(5), 1543–1550.
- Skaugen, T., & Randen, F. (2013). Modeling the spatial distribution of snow water equivalent, taking into account changes in snow-covered area. *Annals of Glaciology*, 54(62), 305–313.
- Skaugen, T., & Weltzien, I. H. (2016). A model for the spatial distribution of snow water equivalent parameterized from the spatial variability of precipitation. *Cryosphere*, 10(5), 1947–1963.
- Skaugen, T., Luijting, H., Saloranta, T., Vikhamar-Schuler, D., & Müller, K. (2018). In search of operational snow model structures for the future - comparing four snowmodels for 17 catchments in Norway. *Hydrology Research*, 49, 6. <https://doi.org/10.2166/nh.2018.198>
- Sturm, M., Liston, G. E., Benson, C., & Holmgren, J. (2001). Characteristics and snow growth of a snowdrift in arctic Alaska. *Arct Antarct Alp Res*, 33, 319–329.
- Sturm, M., McFadden, J. P., Liston, G. E., Chapin, F. C. III, Racine, C. H., & Holmgren, J. (2001). Snow-shrub interactions in arctic tundra: A hypothesis with climatic implications. *Journal of Climate*, 14, 336–344.
- Thomas, I. A., Jordan, P., Shine, O., Fenton, O., Mellander, P. E., Dunlop, P., & Murphy, P. N. C. (2017). Defining optimal DEM resolutions and point densities for modelling hydrologically sensitive areas in agricultural catchments dominated by microtopography. *International Journal of Applied Earth Observation and Geoinformation*, 54, 38–52.
- Trujillo, E., Ramirez, J. A., & Elder, K. J. (2007). Topographic, meteorologic, and canopy controls on the scaling characteristics of the spatial distribution of snow depth fields. *Water Resources Research*, 43, W07409. <https://doi.org/10.1029/2006WR005317>
- Trujillo, E., Ramirez, J. A., & Elder, K. J. (2009). Scaling properties and spatial organization of snow depth fields in sub-alpine forest and alpine tundra. *Hydrological Processes*, 23(11), 1575–1590.
- Veitinger, J., Sovilla, B., & Purves, R. S. (2014). Influence of snow depth distribution on surface roughness in alpine terrain: A multi-scale approach. *Cryosphere*, 8(2), 547–569.
- Winstral, A., Elder, K., & Davis, R. E. (2002). Spatial snow modeling of wind-redistributed snow using terrain-based parameters. *Journal of Hydrometeorology*, 3(5), 524–538.
- Winstral, A., & Marks, D. (2014). Long-term snow distribution observations in a mountain catchment: Assessing variability, time stability, and the representativeness of an index site. *Water Resources Research*, 50, 293–305. <https://doi.org/10.1002/2012WR013038>
- Yevjevich, V. (1972). *Probability and statistics in hydrology*. Littleton, Colorado, USA: Water Resources Publications.
- Zawadzki, I. I. (1973). Statistical properties of precipitation pattern. *Journal of Applied Meteorology*, 12(3), 459–472.